



Marine-derived water-soluble organic nitrogen in coastal air: influence of ocean productivity on atmospheric nitrogen cycling

Jiao Tang^{1,2}, Shujie Hu³, Xiao Wang⁴, Jiaqi Wang⁵, Shaojun Lv², Xiaofei Geng², Guangcai Zhong², Yangzhi Mo², Surat Bualert⁶, Jun Li², Shizhen Zhao², and Gan Zhang²

¹College of Marine Sciences, South China Agricultural University, Guangzhou 510642, China

²State Key Laboratory of Advanced Environmental Technology, Guangzhou Institute of Geochemistry, Chinese Academy of Sciences, Guangzhou 510640, China

³Chongqing Institute of Green and Intelligent Technology, Chinese Academy of Sciences, Chongqing 400714, China

⁴School of Resources and Environment, Henan Polytechnic University, Jiaozuo 454003, China

⁵School of Electrical and Information Engineering, Zhengzhou University, Zhengzhou 450001, China

⁶Faculty of Environment, Kasetsart University, Bangkok 10900, Thailand

Correspondence: Shujie Hu (hushujie@cigit.ac.cn) and Shizhen Zhao (zhaoshizhen@gig.ac.cn)

Received: 27 November 2025 – Discussion started: 16 December 2025

Revised: 19 April 2026 – Accepted: 24 May 2026 – Published: 16 June 2026

Abstract. Organic nitrogen (ON) deposition from aerosols plays a crucial role in oceanic ecosystems; however, the influence of marine biogenic activity on atmospheric ON remains poorly understood. Here, we investigate the contribution of the marine biosphere to water-soluble ON (WSON) in coastal aerosols based on particulate matter samples collected in Bangkok, Thailand, from January 2016 to January 2017. Concentrations of WSON and water-soluble inorganic nitrogen (WSIN, including NO_3^- and NH_4^+) were analyzed and compared across days classified by air mass origin over land as marine-, mixed-, or continental-influenced. Air masses of marine origin showed significantly lower WSON and WSIN concentrations than those from mixed and continental origins. Nevertheless, WSON remained a substantial fraction of water-soluble total nitrogen (WSTN) across all air-mass categories, although the WSON/WSTN ratio alone did not uniquely distinguish marine from anthropogenic influence. Positive matrix factorization revealed that the contribution of sea spray aerosol (SSA)-associated WSON to total WSON increased markedly with oceanic influence, accounting for $3.8\% \pm 6.4\%$, $14\% \pm 14\%$, and $34\% \pm 17\%$ under continental, mixed, and marine conditions, respectively. The corresponding contributions to WSTN were approximately $1.6\% \pm 2.1\%$, $7.3\% \pm 7.6\%$, and $13\% \pm 8.2\%$, with an overall mean of $7.8\% \pm 8.2\%$ over the sampled annual cycle. Moreover, marine productivity, assessed via air mass exposure to chlorophyll *a* concentrations, exhibited a strong positive correlation with SSA-associated WSON ($r = 0.96$, $p < 0.001$), a pattern further supported by large-scale comparison across coastal sites. These results provide multiple lines of evidence that SSA-associated WSON is an important contributor to coastal aerosol WSON under marine influence, with patterns consistent with marine-biogenic enhancement, although anthropogenic co-influences cannot be fully excluded.

1 Introduction

Organic nitrogen (ON), which includes compounds such as amino acids, urea, organic nitrates, nitroaromatics, and humic-like substances, plays an important role in atmospheric processes including air quality, cloud formation, and the nitrogen cycle (Cape et al., 2011). On a global scale, water-soluble ON (WSON) has been estimated to contribute 10%–40% of total airborne ON (Cape et al., 2011; Liu et al., 2021; Matsumoto et al., 2019a), influencing aerosol properties such as solubility, acidity, and hygroscopicity. Furthermore, certain nitrogen-containing organic compounds, including nitroaromatics, have been recognized as important chromophores in brown carbon (He et al., 2022; Liu et al., 2023), thereby influencing radiative forcing. In addition, atmospheric deposition of particulate WSON is increasingly regarded as a significant source of nitrogen input to marine ecosystems (Buchanan et al., 2021; Li et al., 2023).

WSON originates from both direct emissions – including anthropogenic and biogenic sources – and secondary formation through atmospheric reactions (Xu et al., 2020; Yu et al., 2017). These complex sources and atmospheric processes contribute to substantial spatial and temporal variability in WSON deposition (Kanakidou et al., 2012; Li et al., 2023; Yu et al., 2020). Previous studies have identified marine emissions as a notable source of atmospheric ON (Facchini et al., 2008; O'Dowd et al., 2004). Globally, the estimated annual primary emission of soluble ON from the ocean is 2.1 Tg N yr^{-1} , comparable in magnitude to anthropogenic emissions from fossil-fuel combustion and biomass burning (BB) (Ito et al., 2014; Kanakidou et al., 2012). In some remote marine regions, isotopic evidence suggests that aerosol ON can be strongly influenced by marine biological production rather than terrestrial pollution (Altieri et al., 2016).

Recent research has underscored the complexity and variability of WSON in sea spray aerosol (SSA) (Altieri et al., 2012; Li et al., 2019). For instance, primary sea-spray emissions have been recognized as a major source of WSON over the remote Indian sector of the Southern Ocean (Matsumoto et al., 2022). These findings highlight the importance of incorporating marine ON emissions in assessments of net atmospheric WSON deposition, particularly in the open ocean (Luo et al., 2018). However, several field studies in regions strongly influenced by marine air masses have reported only minor contributions from marine-derived WSON – typically below 5% (Leung et al., 2024; Tsagkaraki et al., 2021). This discrepancy highlights the continuing challenge of distinguishing marine from anthropogenic WSON sources in coastal and adjacent marine environments. In this study, we address this issue by combining Positive Matrix Factorization (PMF) source apportionment, air-mass trajectory analysis, a trajectory-based land-retention index, and chlorophyll *a* (Chl *a*) exposure as complementary lines of evidence, while

recognizing that these approaches reduce but do not fully eliminate source ambiguity.

The Indochinese Peninsula (ICP), characterized by high population density and substantial ON deposition (Ito et al., 2014; Kanakidou et al., 2012; Li et al., 2023), provides a suitable context for assessing the influence of marine aerosols on atmospheric WSON. Eutrophication, defined as the excessive enrichment of aquatic systems by nutrients that alters ecosystem structure and function, may enhance primary productivity and potentially promote the emission of ON to the atmosphere (Altieri et al., 2016). Here, we selected Bangkok, the capital of Thailand, which is situated in the central plain of the country and adjacent to the Gulf of Thailand. The region experiences prevailing marine winds from January to October, offering a favorable setting for studying marine aerosol contributions to WSON. Our study aims to: (1) quantify WSON abundances at a coastal site in the ICP; (2) assess marine influences on WSON distributions; and (3) elucidate the mechanisms governing oceanic contributions to WSON.

2 Material and Methods

2.1 Sampling Campaign

A total of 84 total suspended particulate (TSP) samples were collected from the rooftop (57 m above ground level) of the Faculty of Environment at Kasetsart University ($100^{\circ}57' \text{ E}$ and $13^{\circ}85' \text{ N}$; Fig. 1a) in Bangkok, Thailand – a site previously characterized in air quality studies (Tang et al., 2021; Wang et al., 2020). Sampling was conducted over 24 h periods using a high-volume air sampler (flow rate: $0.3 \text{ m}^3 \text{ min}^{-1}$) equipped with pre-combusted quartz-fiber filters (450° C for 6 h). The collection period spanned from 18 January 2016 to 28 January 2017, covering three distinct seasons: Dry I (January–March 2016, $n = 19$), Wet (April–June and October 2016, $n = 35$), and Dry II (November 2016–January 2017, $n = 30$). Sampling frequency averaged $5 \pm 2 \text{ d}$ per month during January–February 2016 and January 2017, with intensified campaigns in March–May and late October–December. Sampling was limited between June and October due to heavy rainfall. Because the sampling frequency varied among seasons and was reduced during the rainy period, this dataset does not represent a uniformly sampled annual climatology. Accordingly, the results are interpreted as observation-based estimates for the sampled annual cycle, and caution is needed when extending them to annual-scale representativeness. Precipitation and solar radiation data were obtained from historical reanalysis products provided by the European Centre for Medium-Range Weather Forecasts (ECMWF). All samples and field blanks were stored in the dark at -20° C until analysis. This storage procedure helps minimize post-collection changes, but it does not eliminate artifacts generated during sampling itself. A summary of TSP mass concentrations, chemical compo-

nents, and meteorological conditions is provided in Table S1 in the Supplement.

2.2 Chemical Analysis

Organic carbon (OC) and elemental carbon (EC) mass concentrations were determined using an OC/EC analyzer following the NIOSH 870 thermal-optical protocol. Inorganic ions (Cl^- , NO_3^- , SO_4^{2-} , Na^+ , K^+ , NH_4^+ , Mg^{2+} , and Ca^{2+}) were quantified by ion chromatography (761 Compact IC, Metrohm, Switzerland), and trace elements were analyzed via inductively coupled plasma–mass spectrometry (ICP–MS; ELAN DRC II, PerkinElmer Ltd., Hong Kong). Analytical errors were 5.5 % for OC, and 3.9 % for EC, below 5.0 % for trace elements, and under 1.0 % for water-soluble ions, based on prior validation (Wang et al., 2020).

Polar molecular tracers – including BB markers (levoglucosan, mannosan, galactosan) and biogenic/anthropogenic secondary organic aerosol (SOA) tracers such as 2-methylglyceric acid (2-MGA), 2-methylthreitol and 2-methylerythritol (2-MGL), 3-methyl-1,2,3-butanetricarboxylic acid (MBTCA), and *o/p*-phthalic acid – were analyzed by gas chromatography–mass spectrometry (GC–MS) following derivatization as previously reported (Geng et al., 2020; Li et al., 2013). The mean recovery of ^{13}C -labeled levoglucosan was $87\% \pm 10\%$. Non-polar tracers of coal and fossil-fuel combustion (hopanes and steranes) were also analyzed, with perdeuterated tetracosane yielding a recovery of $114\% \pm 11\%$ (Wang et al., 2020).

Water-soluble OC (WSOC) and water-soluble total nitrogen (WSTN) were extracted by ultrasonication for 30 min using ultrapure water (resistivity $> 18.2 \text{ M}\Omega \text{ cm}$), followed by filtration through $0.22 \mu\text{m}$ PTFE membranes. Concentrations were measured with a TOC/TN analyzer (model TOC-Vcsh, Shimadzu). WSON was calculated as the difference between WSTN and water-soluble inorganic nitrogen (WSIN), where WSIN comprises $\text{NH}_4^+\text{-N}$, $\text{NO}_3^-\text{-N}$, and $\text{NO}_2^-\text{-N}$: $[\text{WSON}] = [\text{WSTN}] - [\text{WSIN}]$. Nitrite concentrations were consistently below the detection limit of ion chromatography and were excluded from further analysis. It should be noted that some dissolved ON species may not be fully converted to nitrogen monoxide in the TOC/TN analyzer, potentially leading to underestimation of WSON (Miyazaki et al., 2011). Furthermore, integrated filter sampling may be affected by gas–particle sampling artifacts, including volatilization losses of semi-volatile inorganic nitrogen species and possible adsorption of gaseous nitrogen compounds on the filter. Previous studies suggested that adsorption of gaseous organics onto quartz filters may have only a limited effect on WSON measurement under similar sampling conditions, whereas volatilization loss during sampling may still lead to underestimation of particulate WSON (Matsumoto et al., 2014; Matsumoto and Yamato, 2016).

The relative standard deviation (RSD) for WSTN analysis was 3.6 % (method) and 0.77 % (instrument). Method

detection limits were $0.09 \mu\text{g m}^{-3}$ for WSON, $0.03 \mu\text{g m}^{-3}$ for $\text{NO}_3^-\text{-N}$, and $0.02 \mu\text{g m}^{-3}$ for $\text{NH}_4^+\text{-N}$. Field blank levels were $0.067 \mu\text{g N m}^{-3}$ (WSON), $0.043 \mu\text{g N m}^{-3}$ ($\text{NH}_4^+\text{-N}$), and $0.07 \mu\text{g N m}^{-3}$ ($\text{NO}_3^-\text{-N}$), corresponding to average blank-to-sample ratios of 7.1 %, 4.3 %, and 12 %, respectively, consistent with previous reports (Matsumoto et al., 2019a). All reported WSON and WSTN concentrations were blank-corrected and should be interpreted as operationally defined particulate water-soluble N concentrations under the applied sampling protocol.

2.3 Source Apportionment

The U.S. Environmental Protection Agency’s PMF model (PMF 5.0) was employed to perform factor analysis on environmental data with non-negativity constraints and to estimate associated uncertainties (Norris et al., 2014). PMF has been widely applied as a robust tool for aerosol source apportionment. In PMF 5.0, species are evaluated based on the signal-to-noise (S/N) ratio and can be classified as “strong,” “weak,” or “bad”. Weak species are retained but assigned a tripled uncertainty, whereas bad species are excluded from the modeling. In this study, WSON was included as a total variable to resolve its sources. Following the base run, rotational stability (F_{peak}) tests were conducted, and model robustness was evaluated using the base model displacement (DISP), bootstrap (BS), and bootstrap displacement (BS-DISP) methods. A detailed description of PMF procedures is provided in Sect. S1 in the Supplement.

2.4 Air Mass Back Trajectories and Trajectory-Based Chl *a* Exposure

To identify potential source regions, we calculated 120 h back trajectories using the Hybrid Single-particle Lagrangian Integrated Trajectory (HYSPPLIT) model (<http://www.arl.noaa.gov/HYSPPLIT.php>, last access: 11 September 2024), driven by the Global Data Assimilation System (GDAS) meteorological dataset at $1^\circ \times 1^\circ$ resolution (<http://ready.arl.noaa.gov/archives.php>, last access: 4 August 2025). Trajectories were generated at 1 h intervals and subsequently classified through cluster analysis (Fig. 1b and Figs. S1 and S2 in the Supplement). Based on origin and transport pathways, air masses arriving in Bangkok were grouped into six distinct clusters. During the Dry I season, air masses originated predominantly over the Gulf of Thailand/South China Sea (clusters 1–2), with a minor contribution from the Indochina Peninsula (cluster 3). In the Wet season, trajectories were primarily transported via the South China Sea/Gulf of Thailand and the Arabian Sea (clusters 1, 2, 6), whereas Dry II season air masses mainly originated over mainland China and crossed the Indochina Peninsula (clusters 3–5).

Furthermore, the air mass retention ratio over land (R_{land}), defined as the weighted ratio of transport time over land to the total transport duration, was calculated according to the

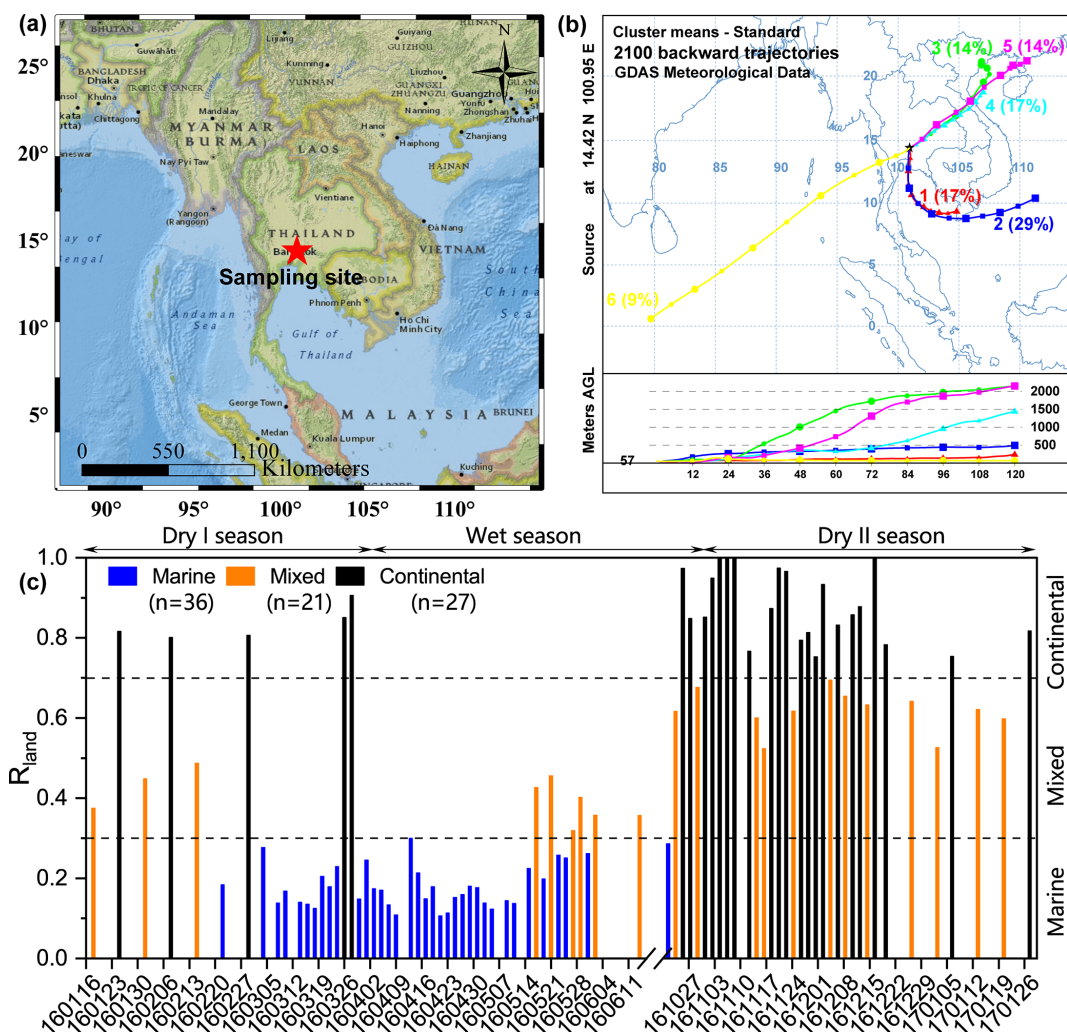


Figure 1. (a) Sampling site location in Bangkok, Thailand. (b) Classified air-mass trajectories (detailed in Figs. S1 and S2). (c) Distribution of R_{land} , with samples categorized as marine-influenced ($R_{land} < 0.3$), mixed-influenced ($0.3 \leq R_{land} \leq 0.7$), or continental-influenced ($R_{land} > 0.7$) based on R_{land} values. The map in panel (a) was created using ArcGIS software with the ESRI National Geographic World Map as the basemap. Sources: Esri, National Geographic, and its data providers; powered by Esri.

method of Zhou et al. (2021, 2023) using Eq. (1). This parameter provides a quantitative measure of terrestrial influence at the receptor site. A schematic illustration is presented in Fig. S3.

$$R_{land} = \frac{\sum_{i=1}^{N_{land}} e^{-t_i/120}}{\sum_{i=1}^{N_{total}} e^{-t_i/120}} \quad (1)$$

Here, N_{total} denotes the total number of trajectory endpoints and N_{land} the number over land. The backward tracking time t_i (in hours) and the weighting factor $e^{-t_i/120}$ account for the diminishing influence of distant regions due to air mass diffusion and particle deposition during transport. As a result, regions associated with longer backward tracking times exert a weaker influence on the receptor site compared to nearby areas. Based on the R_{land} values (Fig. 1c), samples were categorized as marine-influenced ($R_{land} <$

0.3), mixed-influenced ($0.3 \leq R_{land} \leq 0.7$), or continental-influenced ($R_{land} > 0.7$). It should be noted that marine-influenced air masses, as defined by low R_{land} , do not necessarily represent purely marine-biogenic conditions, because aged marine aerosol, shipping emissions, and anthropogenically polluted air masses transported over the ocean may also contribute to aerosol composition. This classification is further supported by molecular marker analysis: during marine-influenced periods, the regression slope for Na^+ versus Mg^{2+} (0.11) closely aligned with the seawater reference ratio (0.12). Elevated levels of Cl^- , Na^+ , Mg^{2+} , and the $\text{Na}^+/\sum \text{ions}$ ratio consistently reflected enhanced sea-salt influence during marine-influenced periods. By contrast, non-sea-salt sulfate (nss-SO_4^{2-}) was not interpreted here as a unique indicator of marine origin, because it may include contributions from both anthropogenic sulfur and ma-

rine biogenic sulfur and may also reflect secondary atmospheric processing during transport (Savoie et al., 2002). Particulate NO_3^- was mainly interpreted as a secondary product formed from the oxidation of NO_x emitted by combustion-related sources, including traffic, shipping, industrial activities, and fossil-fuel combustion or BB, followed by gas-to-particle partitioning or heterogeneous reactions with sea-salt particles during transport (Pryor and Sørensen, 2000). Its concentration was lowest during marine-influenced periods, lower than under mixed- and continental-influenced conditions, a pattern consistent with combustion-derived species such as non-sea-salt K^+ (nss- K^+), EC, and levoglucosan. These results indicate reduced, but not absent, terrestrial and anthropogenic influence during marine-influenced periods (Table S2).

Air mass exposure to Chl *a* (AEC), defined as the mean sea surface Chl *a* concentration along air mass trajectories, was used as a proxy for marine biogenic emissions at the receptor site (Park et al., 2018; Zhou et al., 2023). A statistically significant positive correlation was observed when air masses traveled within the marine boundary layer. However, due to the relatively low correlation between AEC and methanesulfonate, the formulation was adjusted based on the approach of Zhou et al. (2021, 2023), as follows:

$$\text{AEC} = \frac{\sum_{i=1}^{N_{\text{total}}} \text{Chl } a_i \cdot e^{-t_i/120} \cdot e^{-h_i/500}}{n} \quad (2)$$

Here, N_{total} denotes the total number of hourly endpoints (120, including the receptor point) along the trajectory. The variable Chl a_i represents the mean Chl *a* concentration – derived from MODIS-Aqua monthly composites at a 4 km resolution – within a 20 km radius of the i th trajectory endpoint. Endpoints over land were assigned Chl $a_i =$ zero. The weighting factor $e^{-h_i/500}$ accounts for the influence of altitude h_i , reflecting the reduced contribution from higher altitudes due to Chl *a* dilution and particle deposition during transport. The denominator n corresponds to the number of trajectory endpoints with valid Chl *a* data, including zero values over land.

2.5 Potential Source Contribution Function (PSCF) Model

The PSCF model was employed to identify source regions by discretizing the study domain into an $i \times j$ grid. The PSCF values, ranging from 0 to 1, represent the conditional probability that an air parcel passing through a grid cell contributes to high concentrations at the receptor site; elevated values denote a higher probability of source contribution. In this study, PSCF analysis was applied to identify potential geographic source regions of both total WSON and PMF-resolved source categories of WSON in aerosols collected in Bangkok. A detailed description of the PSCF methodology is provided in Sect. S2 and in previous publications (Geng et al., 2020; Tang et al., 2024).

3 Results and Discussion

3.1 Temporal Variations of WSON

Figure S4 and Table S1 present the temporal variations and statistical summaries of meteorological parameters and chemical compositions in TSP throughout the sampling campaign. In Bangkok, Thailand, the mass concentrations of TSP, OC, and EC were $55 \pm 30 \mu\text{g m}^{-3}$ (17–161 $\mu\text{g m}^{-3}$), $12 \pm 6.3 \mu\text{g m}^{-3}$ (3.7–38 $\mu\text{g m}^{-3}$), and $1.4 \pm 0.43 \mu\text{g m}^{-3}$ (0.16–2.8 $\mu\text{g m}^{-3}$), respectively. The TSP levels in this region were substantially lower than those reported in other areas, such as the Eastern Mediterranean ($220 \pm 105 \mu\text{g m}^{-3}$; Tripathee et al., 2021), Jiaozhou Bay ($134 \pm 80 \mu\text{g m}^{-3}$; Xing et al., 2018), and Xi'an during the dust episodes ($2109 \pm 1360 \mu\text{g m}^{-3}$; Wang et al., 2014). Pronounced seasonal variations were observed: TSP levels decreased by 56 % from the Dry I season to the Wet season, but increased by 52 % during the Dry II season. In Bangkok, rainfall during the Wet season (April–October) accounted for 92 % of the annual precipitation total. To examine wet scavenging effects, we evaluated the relationship between TSP concentrations and precipitation (Fig. S5a). A significant negative correlation was identified ($R^2 = 0.21$, $p < 0.001$), consistent with a contribution from wet scavenging, although the relatively low explanatory power indicates that emissions, transport, and precipitation history along the air-mass pathway also substantially influenced TSP variability.

The mass fraction of WSTN in TSP collected in Bangkok averaged $3.8 \% \pm 1.1 \%$ (2.2 %–7.2 %), which was somewhat higher than that reported in the Eastern Mediterranean ($\sim 2.7 \%$; Tripathee et al., 2021) and comparable to values from Sapporo, Japan ($3.8 \% \pm 2.3 \%$; Pavuluri et al., 2015). As shown in Fig. 2a and Table S2, the concentrations of the individual WSTN components, including WSON, NO_3^- -N, and NH_4^+ -N, were $0.95 \pm 0.40 \mu\text{g N m}^{-3}$ (0.27–2.3 $\mu\text{g N m}^{-3}$), $0.60 \pm 0.52 \mu\text{g N m}^{-3}$ (below detection limitation (BDL)–2.7 $\mu\text{g N m}^{-3}$), and $0.47 \pm 0.44 \mu\text{g N m}^{-3}$ (BDL–2.2 $\mu\text{g N m}^{-3}$), respectively. WSON correlated positively with both TSP ($r = 0.65$, $p < 0.01$) and WSIN ($r = 0.51$, $p < 0.01$) (Fig. S6), indicating that WSON variability was linked to overall aerosol loading and co-varied with inorganic N across the dataset.

Concentrations of WSON, NO_3^- -N, NH_4^+ -N, TSP, OC, and EC varied considerably under different air mass regimes (Table S2). The nonparametric Mann–Whitney U test indicated that WSON and NO_3^- -N levels were significantly lower during marine-influenced periods than under mixed or continental conditions (Fig. 2c, $p < 0.001$). In contrast, NH_4^+ -N concentrations were slightly higher during marine periods. This contrast indicates that the responses of individual N species were not uniform across air-mass regimes and should not be attributed to a single dominant source. This aligns with earlier studies reporting that aerosols in remote marine regions may still be substantially influenced by conti-

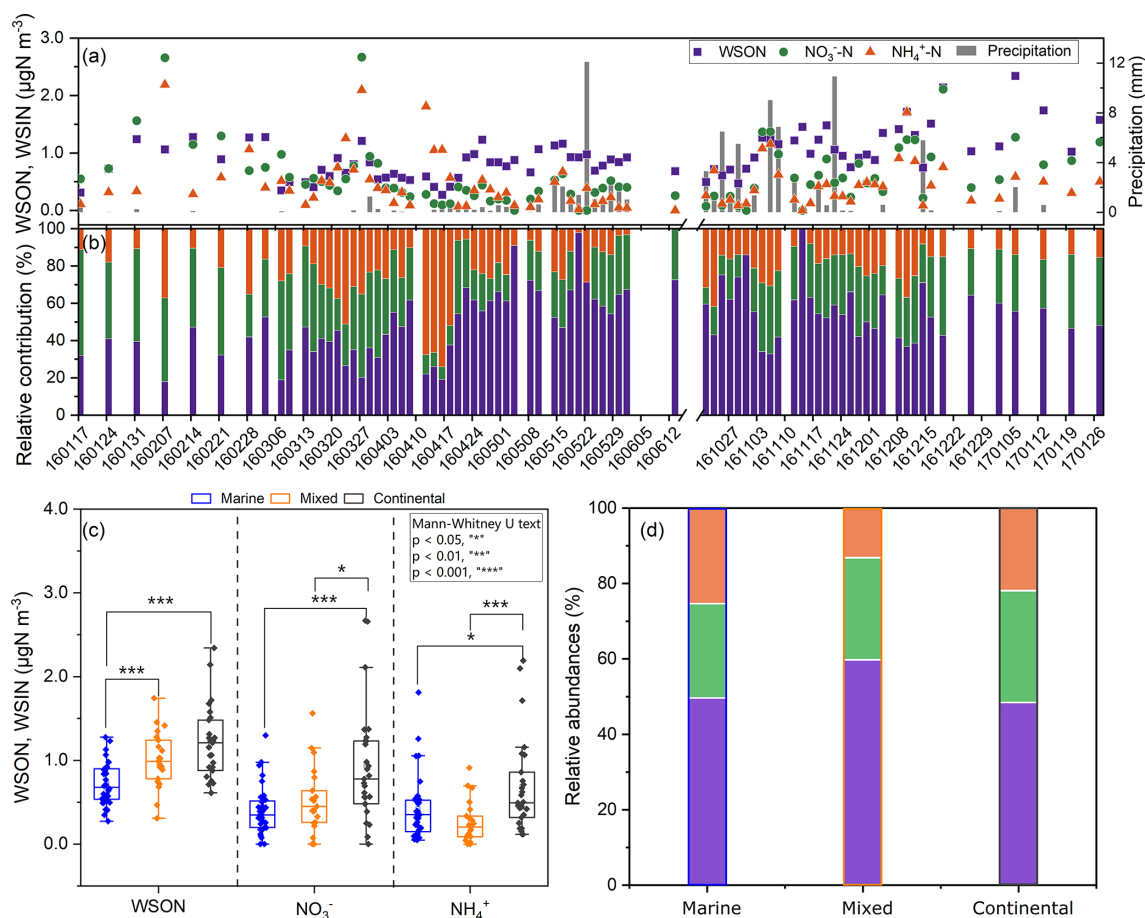


Figure 2. Temporal variations and source influences on N species in Bangkok aerosols. **(a)** Time-series of concentrations of WSON and WSIN ($\text{NH}_4^+\text{-N}$, $\text{NO}_3^-\text{-N}$), overlaid with daily rainfall from ECMWF reanalysis data. **(b)** Relative contributions of WSON and WSIN to WSTN across the study period. **(c)** Concentration distributions and **(d)** relative abundances of WSON and WSIN during marine-, mixed-, and continental-influenced periods.

mental inputs (Jickells et al., 2013). BB tracers (e.g., levoglucosan, galactosan, mannosan) were also significantly lower during marine-influenced days (see Table S2). Furthermore, WSON correlated with BB and SOA markers and aerosol liquid water content (ALWC, Sect. S3) under mixed and continental conditions, whereas these associations were not evident during marine periods (Fig. S7). Taken together, these patterns suggest that the lower WSON concentrations during marine-influenced periods likely reflected a combination of reduced continental and combustion-related influence, differences in transport history, and atmospheric processing. Seasonally higher rainfall may also have contributed, but because no significant direct correlation was found between WSON and precipitation (Fig. S5b), precipitation alone cannot explain the observed WSON variability.

The WSON/WSTN ratio during marine-influenced days ($50\% \pm 17\%$) was similar to that under continental influence ($48\% \pm 15\%$) but lower than during mixed conditions ($60\% \pm 17\%$) (Fig. 2d). This pattern shows that the WSON/WSTN ratio alone may not be a reliable way to

identify WSON source in this dataset. The elevated ratio under mixed conditions likely reflects overlapping marine and continental influences together with different responses of WSON and WSIN to transport and removal processes, rather than a unique source type. During marine-influenced periods, WSON may reflect both marine-related contributions and anthropogenic inputs associated with shipping emissions and atmospheric processing, whereas continental periods are more strongly affected by terrestrial anthropogenic emissions. Precipitation may alter the WSON/WSTN ratio through differential scavenging: WSIN species (e.g., NO_3^- , NH_4^+) are efficiently removed by rainfall (Matsumoto et al., 2019b; Nehir and Koçak, 2018), as WSIN showed stronger correlations with precipitation (Fig. S5c and d). By contrast, the absence of a significant WSON–precipitation correlation indicates that WSON variability in this dataset was less directly coupled to precipitation, rather than supporting a distinct scavenging mechanism.

Annually, WSON accounted for $52\% \pm 17\%$ of the WSTN (Fig. 2b) – substantially higher than values re-

ported from a forest site ($20\% \pm 11\%$; Miyazaki et al., 2014), an offshore island (27% ; Tian et al., 2023), Saproporo ($9.2\% \pm 7.3\%$; Pavuluri et al., 2015), and coastal Qingdao ($\sim 20\%$; Shi et al., 2010). Elevated WSON/WSTN ratios have been documented in source emissions such as BB ($80\% \pm 6.3\%$), vehicle exhaust ($67\% \pm 16\%$), and shipping emissions ($54\% \pm 31\%$) (Yu et al., 2017), as well as receptor regions such as Hawaii (64% ; Cornell et al., 2001) and polluted continental urban regions such as Xi'an (45% , range: $22\%–68\%$; Ho et al., 2015). By comparison, the South China Sea, which is more strongly influenced by open-marine conditions, exhibited a WSON/WSTN ratio of 34% , whereas the Yellow Sea, subject to stronger continental and anthropogenic influence, showed a lower ratio of 17% (Shi et al., 2010). During phytoplankton blooms, ON can dominate aerosol composition, contributing up to 84% of WSTN (Violaki et al., 2015) and 63% of submicrometer aerosol mass (O'Dowd et al., 2004). Collectively, these studies indicate that elevated WSON/WSTN ratios may arise from anthropogenic combustion sources, shipping emissions, marine-related emissions, and secondary atmospheric processing. Therefore, the WSON/WSTN ratio alone is insufficient to discriminate marine-biogenic, shipping-related, and continental anthropogenic sources of WSON. More quantitative approaches are needed to apportion the origins of aerosol ON.

3.2 SSA as a Major WSON Source in Marine-influenced Days

To elucidate the contributions of marine and anthropogenic sources to WSON in this coastal urban environment, we applied the PMF 5.0 model to 84 aerosol samples characterized by 26 chemical species. The model resolved WSON into seven source factors: shipping emissions, secondary sulfate, dust, SOA, BB, vehicle emissions and fossil-fuel combustion (VEFC), and SSA (Fig. S8); the detailed identification of each factor is provided in Sect. S1. The SSA factor was characterized primarily by high loadings of Na^+ , Cl^- , and Mg^{2+} , with WSON also contributing to this factor. We therefore interpret this factor as a sea-salt-associated aerosol carrying WSON, rather than as purely biogenic aerosol. Furthermore, PSCF mapping of SSA-associated WSON pointed mainly to the Gulf of Thailand and, to a lesser extent, the Bay of Bengal (see Fig. S10), supporting the importance of marine-related source regions for this factor.

Over the entire study period, SOA ($34\% \pm 25\%$), VEFC ($21\% \pm 16\%$), SSA ($19\% \pm 19\%$), and BB ($13\% \pm 12\%$) emerged as the dominant sources of WSON in Bangkok aerosols (Figs. 3b and S9). This is consistent with previous reports highlighting secondary formation and BB as major contributors to WSON (Leung et al., 2024; Tsagkaraki et al., 2021; Yu et al., 2017). Earlier factor-based studies also indicated that sea salt can explain over 20% of the variance in WSON (Chen and Chen, 2010; Shi et al., 2010). The con-

tribution of SSA in our study, however, exceeded values reported for other coastal regions such as Hong Kong (4.4%) and the Eastern Mediterranean ($< 5\%$) (Leung et al., 2024; Nehir and Koçak, 2018; Tsagkaraki et al., 2021). Two factors may explain this discrepancy. First, ON in coarse aerosols often originates from soil, dust, or large sea-salt particles (Cornell et al., 2001; Mace et al., 2003), whereas studies focusing on $\text{PM}_{2.5}$ – such as those in Hong Kong – naturally record lower sea-salt contributions (Leung et al., 2024). Second, the ultra-oligotrophic marine environment of the Eastern Mediterranean, characterized by low nutrient availability and limited riverine input, results in low marine productivity and thus diminished marine-derived WSON (Nehir and Koçak, 2018; Tsagkaraki et al., 2021).

We further disaggregated WSON source contributions by air mass regime (Fig. 3b). Under marine influence, SSA constituted the dominant source of WSON ($34\% \pm 17\%$), exceeding SOA ($19\% \pm 17\%$), VEFC ($19\% \pm 14\%$), and secondary sulfate ($17\% \pm 16\%$), while BB contributed minimally ($7.1\% \pm 6.0\%$). This pattern is consistent with studies conducted in remote marine and island settings (Altieri et al., 2016; Miyazaki et al., 2011; Violaki et al., 2015). Under mixed marine–continental influence, SOA became the dominant contributor ($51\% \pm 20\%$), followed by VEFC ($19\% \pm 15\%$) and SSA ($14\% \pm 15\%$). During continental conditions, SOA remained the primary source ($41\% \pm 26\%$), likely reflecting multiple secondary formation pathways of nitrogen-containing organic aerosol, of which nitroaromatics may represent one possible subset of these compounds (Xie et al., 2017). Previous work has shown that oxidized α -pinene SOA can account for $33\%–38\%$ of WSON, with aerosol liquid water further promoting nighttime secondary WSON formation (Xu et al., 2020). Under continental regimes, VEFC ($26\% \pm 19\%$) and BB ($23\% \pm 14\%$) also contributed substantially to WSON. Notably, the SSA contribution dropped sharply to $3.8\% \pm 6.4\%$ under continental influence. Expressed relative to total WSTN, SSA-associated WSON contributed approximately $1.6\% \pm 2.1\%$, $7.3\% \pm 7.6\%$, and $13\% \pm 8.2\%$ under continental-, mixed-, and marine-influenced conditions, respectively, with an overall mean contribution of $7.8\% \pm 8.2\%$ over the sampled annual cycle, further illustrating its enhanced importance during marine influence.

Temporal variations in source-resolved WSON concentrations are shown in Fig. 3a. Among the three air mass regimes, SSA-associated WSON concentrations peaked under marine influence ($0.19 \pm 0.12 \mu\text{g N m}^{-3}$), approximately 1.7 times higher than during mixed periods ($0.11 \pm 0.12 \mu\text{g N m}^{-3}$) and five times higher than during continental periods ($0.037 \pm 0.069 \mu\text{g N m}^{-3}$). Shipping-emission-associated WSON was also elevated during marine days ($0.015 \pm 0.0075 \mu\text{g N m}^{-3}$) relative to mixed and continental periods, though its overall contribution remained low ($\sim 3\%$). WSON associated with the secondary sulfate factor under marine influence ($0.094 \pm 0.086 \mu\text{g N m}^{-3}$)

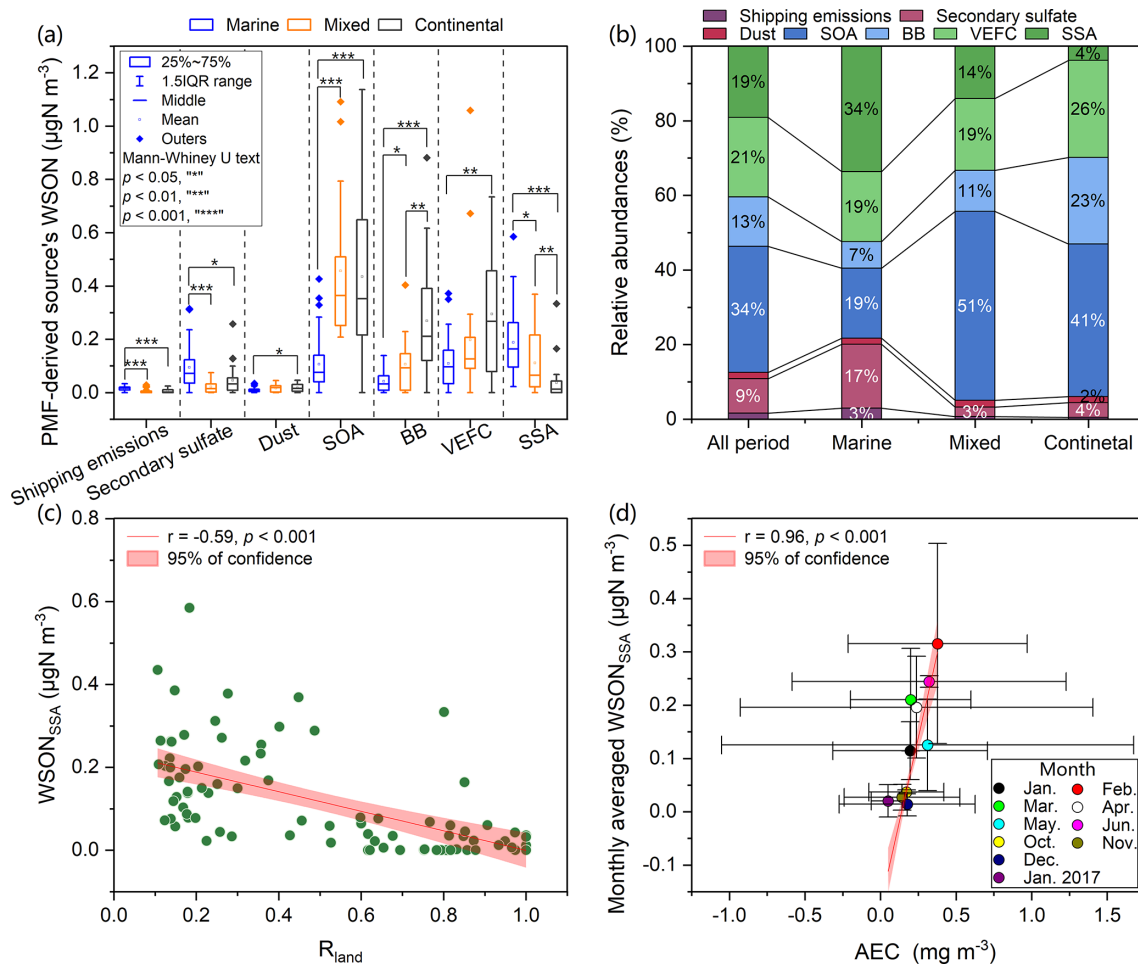


Figure 3. Source apportionment of WSON based on PMF. **(a)** Absolute concentrations and **(b)** relative contributions of PMF-resolved sources to total WSON during the entire study period and under marine-, mixed-, and continental-influenced conditions. **(c)** Correlation between R_{land} and SSA-associated WSON. **(d)** Relationship between AEC and monthly averaged SSA-associated WSON concentrations, color-coded by sampling month.

was significantly higher than during mixed periods ($0.022 \pm 0.023 \mu\text{gN m}^{-3}$) and during continental periods ($0.046 \pm 0.056 \mu\text{gN m}^{-3}$), consistent with an important contribution from secondary inorganic aerosol formation. Although the PMF-resolved shipping factor remained low during marine-influenced periods, other anthropogenic-related factors, including secondary sulfate, VEFC and SOA, still showed non-negligible contributions, consistent with the view that marine-influenced air masses in this study should not be interpreted as purely marine-biogenic conditions. These results also indicate that marine air mass transport plays an important role in the enhancement of SSA-associated WSON, further supported by a strong negative correlation between SSA-associated WSON and R_{land} (Fig. 3c, $r = -0.59$, $p < 0.001$). In contrast, SOA-, BB-, and VEFC-associated WSON increased significantly under mixed and continental conditions. Although SOA is generally considered more susceptible to wet removal than pri-

mary aerosol (Sun et al., 2011; Zhao et al., 2026), no significant correlation was observed between precipitation and PMF-resolved source concentrations in this dataset. This suggests that wet scavenging alone did not dominate the observed source-resolved WSON variability.

3.3 Marine Productivity as a Key Factor Influencing Coastal WSON Distribution

SSA is dominated by inorganic sea salt but can also comprise an important organic fraction derived from ocean-surface materials (Prather et al., 2013; Quinn et al., 2014; Schiffer et al., 2018). Previous studies have linked marine biological productivity to the organic enrichment of SSA (O'Dowd et al., 2015; Violaki et al., 2015), and Chl *a* has often been used as a broad proxy for ocean-surface biological conditions (Facchini et al., 2008; O'Dowd et al., 2004). Given the substantial contribution of SSA-associated WSON to to-

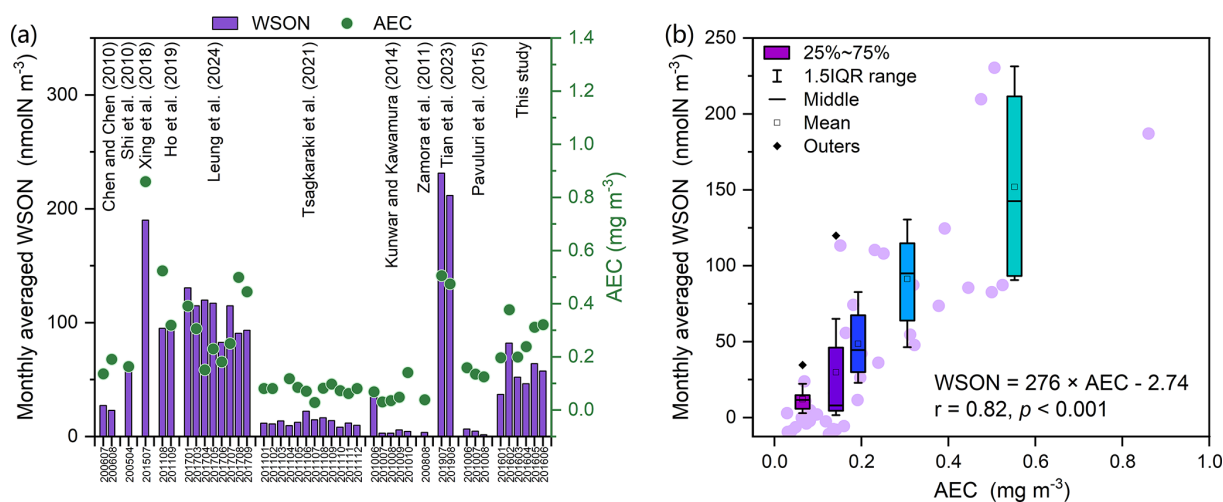


Figure 4. (a) Geographic distributions and (b) correlation between AEC values and monthly mean WSON concentration in coastal regions predominantly influenced by marine air masses. Values are provided in Table S3. Air mass trajectories for these coastal and island sampling sites were recalculated using the HYSPLIT model, and AEC values were derived from MODIS monthly Chl *a* concentrations.

tal WSON and WSTN during marine-influenced periods in our study, we further examined whether marine productivity was related to its variability.

We calculated AEC values based on monthly MODIS Chl *a* data (4 km resolution) along 120 h backward trajectories (see Methods). SSA-associated WSON exhibited a strong positive correlation with AEC ($r = 0.96$, $p < 0.001$; Fig. 3d), consistent with a linkage between marine productivity and the variability of this factor. This contrasts with Tian et al. (2023), who observed significant WSON-AEC correlations only in summer, likely reflecting stronger anthropogenic influences and/or weaker marine signals during other seasons. While previous multivariate regression identified wind speed and Chl *a* as key predictors of the organic fraction in SSA (Gantt et al., 2011), other studies note that Chl *a* alone may not fully capture organic enrichment (Rinaldi et al., 2013). Still, moderate correlations ($r \approx 0.60$) between Chl *a* and marine organic aerosol abundance have been reported (Sciare et al., 2009). However, AEC may also covary with marine transport conditions, meteorology, and other seasonally structured processes, and correlation alone does not establish source dominance. Taken together, the PMF results, reduced terrestrial influence, and the positive AEC relationship are consistent with an important marine-biogenic enhancement of SSA-associated WSON during marine-influenced periods, although shipping and other anthropogenic co-influences cannot be fully excluded.

To further examine the broader relevance of this relationship, we compiled a dataset of WSON concentrations from coastal and island sites and recalculated air-mass trajectories, R_{land} , and AEC values based on MODIS Chl *a* for each site (Fig. 4a and Table S3). Across these marine-influenced coastal datasets, the highest WSON concentrations occurred at Huaniao Island (Tian et al., 2023), fol-

lowed by Jiaozhou Bay (Xing et al., 2018), Hong Kong (Ho et al., 2019; Leung et al., 2024), the South China Sea (Shi et al., 2010), and Bangkok. The lowest values were observed in the Eastern Mediterranean (Tsagkaraki et al., 2021), Keelung City (Chen and Chen, 2010), Okinawa Island (Kunwar and Kawamura, 2014), Barbados (Zamora et al., 2011), and Sapporo (Pavuluri et al., 2015). Notably, spatial patterns in AEC closely mirrored those in WSON. A significant positive correlation was found between WSON and AEC across all sites ($r = 0.82$, $\text{WSON} [\text{nmol m}^{-3}] = 276 \times \text{AEC} [\text{mg m}^{-3}] - 2.74$, Fig. 4b). This large-scale comparison supports the broader consistency of the observed relationship, although the influence of site-to-site differences in sampling protocol, aerosol size fraction, and anthropogenic impact cannot be excluded.

4 Conclusions

The equation derived in this study ($\text{WSON} [\text{nmol m}^{-3}] = 276 \times \text{AEC} [\text{mg m}^{-3}] - 2.74$) provides an empirical basis for examining the linkage between coastal aerosol water-soluble organic nitrogen (WSON) and oceanic biological conditions along air-mass transport pathways. Our results indicate that sea spray aerosol (SSA)-associated WSON is an important contributor to coastal aerosol WSON under marine-influenced conditions, and its covariation with trajectory-based air-mass exposure to chlorophyll *a* (Chl *a*) (AEC) is consistent with marine-biogenic enhancement. However, these implications should be interpreted with caution because the present dataset was obtained with seasonally uneven sampling coverage, 24 h integrated filter sampling, and without isotopic constraints that could more directly distinguish marine-biogenic, shipping-related, and continental anthropogenic sources. Future work combining more tempo-

rally uniform observations with isotopic and molecular-level characterization is needed to further strengthen source attribution. We therefore suggest that integrating satellite-derived Chl *a* data into air mass trajectory analyses may help improve future assessments of marine-related WSON variability.

Code and data availability. The analysis outputs and code used in this study are publicly available from the Open Science Framework (OSF) repository at <https://doi.org/10.17605/OSF.IO/YMJ3F> (Tang, 2026).

Supplement. The supplement related to this article is available online at <https://doi.org/10.5194/acp-26-8341-2026-supplement>.

Author contributions. Conceptualization: JT. Funding acquisition: JT, SH, SZ, and GaZ. Investigation: JT, XW, JW, SL, XG, GuZ, and SB. Methodology: JT, XW, and JW. Project administration: GaZ and SZ. Resources: YM, SZ, JL, and GaZ. Software: XW and SL. Supervision: JL, SZ, and GaZ. Validation: JT and SZ. Writing (original draft): JT. Writing (review and editing): XW, SH, SZ, and GaZ.

Competing interests. The contact author has declared that none of the authors has any competing interests.

Disclaimer. Publisher's note: Copernicus Publications remains neutral with regard to jurisdictional claims made in the text, published maps, institutional affiliations, or any other geographical representation in this paper. The authors bear the ultimate responsibility for providing appropriate place names. Views expressed in the text are those of the authors and do not necessarily reflect the views of the publisher.

Acknowledgements. The authors thank the editor, the anonymous reviewers, and all colleagues who provided constructive comments and practical support during manuscript preparation and publication.

Financial support. This research has been supported by the National Natural Science Foundation of China (grant nos. 442192511 and 42473070), the Guangdong Basic and Applied Basic Research Foundation (grant nos. 2023B0303000007 and 2023B1515020067), and the National Science Foundation of Chongqing (grant no. CSTB2024NSCQ-MSX0897).

Review statement. This paper was edited by Sergio Rodríguez and reviewed by two anonymous referees.

References

- Altieri, K. E., Hastings, M. G., Peters, A. J., and Sigman, D. M.: Molecular characterization of water soluble organic nitrogen in marine rainwater by ultra-high resolution electrospray ionization mass spectrometry, *Atmos. Chem. Phys.*, 12, 3557–3571, <https://doi.org/10.5194/acp-12-3557-2012>, 2012.
- Altieri, K. E., Fawcett, S. E., Peters, A. J., Sigman, D. M., and Hastings, M. G.: Marine biogenic source of atmospheric organic nitrogen in the subtropical North Atlantic, *P. Natl. Acad. Sci. USA*, 113, 925–930, <https://doi.org/10.1073/pnas.1516847113>, 2016.
- Buchanan, P. J., Aumont, O., Bopp, L., Mahaffey, C., and Tagliabue, A.: Impact of intensifying nitrogen limitation on ocean net primary production is fingerprinted by nitrogen isotopes, *Nat. Commun.*, 12, 6214, <https://doi.org/10.1038/s41467-021-26552-w>, 2021.
- Cape, J. N., Cornell, S. E., Jickells, T. D., and Nemitz, E.: Organic nitrogen in the atmosphere – Where does it come from? A review of sources and methods, *Atmos. Res.*, 102, 30–48, <https://doi.org/10.1016/j.atmosres.2011.07.009>, 2011.
- Chen, H.-Y. and Chen, L.-D.: Occurrence of water soluble organic nitrogen in aerosols at a coastal area, *J. Atmos. Chem.*, 65, 49–71, <https://doi.org/10.1007/s10874-010-9181-y>, 2010.
- Cornell, S., Mace, K., Coeppicus, S., Duce, R., Huebert, B., Jickells, T., and Zhuang, L. Z.: Organic nitrogen in Hawaiian rain and aerosol, *J. Geophys. Res.-Atmos.*, 106, 7973–7983, <https://doi.org/10.1029/2000jd900655>, 2001.
- Facchini, M. C., Decesari, S., Rinaldi, M., Carbone, C., Finessi, E., Mircea, M., Fuzzi, S., Moretti, F., Tagliavini, E., Ceburnis, D., and O'Dowd, C. D.: Important Source of Marine Secondary Organic Aerosol from Biogenic Amines, *Environ. Sci. Technol.*, 42, 9116–9121, <https://doi.org/10.1021/es8018385>, 2008.
- Gantt, B., Meskhidze, N., Facchini, M. C., Rinaldi, M., Ceburnis, D., and O'Dowd, C. D.: Wind speed dependent size-resolved parameterization for the organic mass fraction of sea spray aerosol, *Atmos. Chem. Phys.*, 11, 8777–8790, <https://doi.org/10.5194/acp-11-8777-2011>, 2011.
- Geng, X., Mo, Y., Li, J., Zhong, G., Tang, J., Jiang, H., Ding, X., Malik, R. N., and Zhang, G.: Source apportionment of water-soluble brown carbon in aerosols over the northern South China Sea: Influence from land outflow, SOA formation and marine emission, *Atmos. Environ.*, 229, 117484, <https://doi.org/10.1016/j.atmosenv.2020.117484>, 2020.
- He, Q., Li, C., Siemens, K., Morales, A. C., Hettiyadura, A. P. S., Laskin, A., and Rudich, Y.: Optical Properties of Secondary Organic Aerosol Produced by Photooxidation of Naphthalene under NO_x Condition, *Environ. Sci. Technol.*, 56, 4816–4827, <https://doi.org/10.1021/acs.est.1c07328>, 2022.
- Ho, K. F., Ho, S. S. H., Huang, R.-J., Liu, S. X., Cao, J.-J., Zhang, T., Chuang, H.-C., Chan, C. S., Hu, D., and Tian, L.: Characteristics of water-soluble organic nitrogen in fine particulate matter in the continental area of China, *Atmos. Environ.*, 106, 252–261, <https://doi.org/10.1016/j.atmosenv.2015.02.010>, 2015.
- Ho, S. S. H., Li, L., Qu, L., Cao, J., Lui, K. H., Niu, X., Lee, S.-C., and Ho, K. F.: Seasonal behavior of water-soluble organic nitrogen in fine particulate matter (PM_{2.5}) at urban coastal environments in Hong Kong, *Air Qual. Atmos. Hlth.*, 12, 389–399, <https://doi.org/10.1007/s11869-018-0654-5>, 2019.

- Ito, A., Lin, G., and Penner, J. E.: Reconciling modeled and observed atmospheric deposition of soluble organic nitrogen at coastal locations, *Global Biogeochem. Cy.*, 28, 617–630, <https://doi.org/10.1002/2013GB004721>, 2014.
- Jickells, T., Baker, A. R., Cape, J. N., Cornell, S. E., and Nemitz, E.: The cycling of organic nitrogen through the atmosphere, *Philos. T. Roy. Soc. B*, 368, <https://doi.org/10.1098/rstb.2013.0115>, 2013.
- Kanakidou, M., Duce, R. A., Prospero, J. M., Baker, A. R., Benitez-Nelson, C., Dentener, F. J., Hunter, K. A., Liss, P. S., Mahowald, N., Okin, G. S., Sarin, M., Tsigaridis, K., Uematsu, M., Zamora, L. M., and Zhu, T.: Atmospheric fluxes of organic N and P to the global ocean, *Global Biogeochem. Cy.*, 26, <https://doi.org/10.1029/2011gb004277>, 2012.
- Kunwar, B. and Kawamura, K.: One-year observations of carbonaceous and nitrogenous components and major ions in the aerosols from subtropical Okinawa Island, an outflow region of Asian dusts, *Atmos. Chem. Phys.*, 14, 1819–1836, <https://doi.org/10.5194/acp-14-1819-2014>, 2014.
- Leung, C. W., Wang, X., and Hu, D.: Characteristics and source apportionment of water-soluble organic nitrogen (WSON) in PM_{2.5} in Hong Kong: With focus on amines, urea, and nitroaromatic compounds, *J. Hazard. Mater.*, 469, 133899, <https://doi.org/10.1016/j.jhazmat.2024.133899>, 2024.
- Li, J. J., Wang, G. H., Cao, J. J., Wang, X. M., and Zhang, R. J.: Observation of biogenic secondary organic aerosols in the atmosphere of a mountain site in central China: temperature and relative humidity effects, *Atmos. Chem. Phys.*, 13, 11535–11549, <https://doi.org/10.5194/acp-13-11535-2013>, 2013.
- Li, R., Cui, L., Zhao, Y., Fu, H., Li, Q., Zhang, L., and Chen, J.: Size-segregated water-soluble N-bearing species in the land-sea boundary zone of East China, *Atmos. Environ.*, 218, 116990, <https://doi.org/10.1016/j.atmosenv.2019.116990>, 2019.
- Li, Y., Fu, T.-M., Yu, J. Z., Yu, X., Chen, Q., Miao, R., Zhou, Y., Zhang, A., Ye, J., Yang, X., Tao, S., Liu, H., and Yao, W.: Dissecting the contributions of organic nitrogen aerosols to global atmospheric nitrogen deposition and implications for ecosystems, *Natl. Sci. Rev.*, 10, <https://doi.org/10.1093/nsr/nwad244>, 2023.
- Liu, Q., Liu, Y., Zhao, Q., Zhang, T., and Schauer, J. J.: Increases in the formation of water soluble organic nitrogen during Asian dust storm episodes, *Atmos. Res.*, 253, 105486, <https://doi.org/10.1016/j.atmosres.2021.105486>, 2021.
- Liu, X., Wang, H., Wang, F., Lv, S., Wu, C., Zhao, Y., Zhang, S., Liu, S., Xu, X., Lei, Y., and Wang, G.: Secondary Formation of Atmospheric Brown Carbon in China Haze: Implication for an Enhancing Role of Ammonia, *Environ. Sci. Technol.*, 57, 11163–11172, <https://doi.org/10.1021/acs.est.3c03948>, 2023.
- Luo, L., Kao, S.-J., Bao, H., Xiao, H., Xiao, H., Yao, X., Gao, H., Li, J., and Lu, Y.: Sources of reactive nitrogen in marine aerosol over the Northwest Pacific Ocean in spring, *Atmos. Chem. Phys.*, 18, 6207–6222, <https://doi.org/10.5194/acp-18-6207-2018>, 2018.
- Mace, K. A., Duce, R. A., and Tindale, N. W.: Organic nitrogen in rain and aerosol at Cape Grim, Tasmania, Australia, *J. Geophys. Res.-Atmos.*, 108, <https://doi.org/10.1029/2002JD003051>, 2003.
- Matsumoto, K. and Yamato, K.: Uncertainties in the measurements of water-soluble organic nitrogen in the aerosol, *Atmos. Environ.*, 144, 220–225, <https://doi.org/10.1016/j.atmosenv.2016.08.061>, 2016.
- Matsumoto, K., Yamamoto, Y., Kobayashi, H., Kaneyasu, N., and Nakano, T.: Water-soluble organic nitrogen in the ambient aerosols and its contribution to the dry deposition of fixed nitrogen species in Japan, *Atmos. Environ.*, 95, 334–343, <https://doi.org/10.1016/j.atmosenv.2014.06.037>, 2014.
- Matsumoto, K., Sakata, K., and Watanabe, Y.: Water-soluble and water-insoluble organic nitrogen in the dry and wet deposition, *Atmos. Environ.*, 218, <https://doi.org/10.1016/j.atmosenv.2019.117022>, 2019a.
- Matsumoto, K., Watanabe, Y., Horiuchi, K., and Nakano, T.: Simultaneous measurement of the water-soluble organic nitrogen in the gas phase and aerosols at a forested site in Japan, *Atmos. Environ.*, 200, 312–318, <https://doi.org/10.1016/j.atmosenv.2018.12.011>, 2019b.
- Matsumoto, K., Kobayashi, H., Hara, K., Ishino, S., and Hayashi, M.: Water-soluble organic nitrogen in fine aerosols over the Southern Ocean, *Atmos. Environ.*, 287, <https://doi.org/10.1016/j.atmosenv.2022.119287>, 2022.
- Miyazaki, Y., Kawamura, K., Jung, J., Furutani, H., and Uematsu, M.: Latitudinal distributions of organic nitrogen and organic carbon in marine aerosols over the western North Pacific, *Atmos. Chem. Phys.*, 11, 3037–3049, <https://doi.org/10.5194/acp-11-3037-2011>, 2011.
- Miyazaki, Y., Fu, P., Ono, K., Tachibana, E., and Kawamura, K.: Seasonal cycles of water-soluble organic nitrogen aerosols in a deciduous broadleaf forest in northern Japan, *J. Geophys. Res.-Atmos.*, 119, 1440–1454, <https://doi.org/10.1002/2013jd020713>, 2014.
- Nehir, M. and Koçak, M.: Atmospheric water-soluble organic nitrogen (WSON) in the eastern Mediterranean: origin and ramifications regarding marine productivity, *Atmos. Chem. Phys.*, 18, 3603–3618, <https://doi.org/10.5194/acp-18-3603-2018>, 2018.
- Norris, G., Duvall, R., Brown, S., and Bai, S.: EPA Positive Matrix Factorization (PMF) 5.0 Fundamentals and User Guide, EPA/600/R-14/108, U.S. Environmental Protection Agency Office of Research and Development, Washington, DC, 2014.
- O'Dowd, C., Ceburnis, D., Ovadnevaite, J., Bialek, J., Stengel, D. B., Zacharias, M., Nitschke, U., Connan, S., Rinaldi, M., Fuzzi, S., Decesari, S., Cristina Facchini, M., Marullo, S., Santoluni, R., Dell'Anno, A., Corinaldesi, C., Tangherlini, M., and Danovaro, R.: Connecting marine productivity to sea-spray via nanoscale biological processes: Phytoplankton Dance or Death Disco?, *Sci. Rep.-UK*, 5, 14883, <https://doi.org/10.1038/srep14883>, 2015.
- O'Dowd, C. D., Facchini, M. C., Cavalli, F., Ceburnis, D., Mircea, M., Decesari, S., Fuzzi, S., Yoon, Y. J., and Putaud, J.-P.: Biogenically driven organic contribution to marine aerosol, *Nature*, 431, 676–680, <https://doi.org/10.1038/nature02959>, 2004.
- Park, K.-T., Lee, K., Kim, T.-W., Yoon, Y. J., Jang, E.-H., Jang, S., Lee, B.-Y., and Hermansen, O.: Atmospheric DMS in the Arctic Ocean and Its Relation to Phytoplankton Biomass, *Global Biogeochem. Cy.*, 32, 351–359, <https://doi.org/10.1002/2017GB005805>, 2018.
- Pavuluri, C. M., Kawamura, K., and Fu, P. Q.: Atmospheric chemistry of nitrogenous aerosols in northeastern Asia: biological sources and secondary formation, *Atmos. Chem. Phys.*, 15, 9883–9896, <https://doi.org/10.5194/acp-15-9883-2015>, 2015.
- Prather, K. A., Bertram, T. H., Grassian, V. H., Deane, G. B., Stokes, M. D., DeMott, P. J., Aluwihare, L. I., Palenik, B. P., Azam, F., Seinfeld, J. H., Moffet, R. C., Molina, M. J.,

- Cappa, C. D., Geiger, F. M., Roberts, G. C., Russell, L. M., Ault, A. P., Baltrusaitis, J., Collins, D. B., Corrigan, C. E., Cuadra-Rodriguez, L. A., Ebben, C. J., Forestieri, S. D., Guasco, T. L., Hersey, S. P., Kim, M. J., Lambert, W. F., Modini, R. L., Mui, W., Pedler, B. E., Ruppel, M. J., Ryder, O. S., Schoepp, N. G., Sullivan, R. C., and Zhao, D.: Bringing the ocean into the laboratory to probe the chemical complexity of sea spray aerosol, *P. Natl. Acad. Sci. USA*, 110, 7550–7555, <https://doi.org/10.1073/pnas.1300262110>, 2013.
- Pryor, S. C. and Sørensen, L. L.: Nitric Acid–Sea Salt Reactions: Implications for Nitrogen Deposition to Water Surfaces, *J. Appl. Meteorol.*, 39, 725–731, <https://doi.org/10.1175/1520-0450.39.5.725>, 2000.
- Quinn, P. K., Bates, T. S., Schulz, K. S., Coffman, D. J., Frossard, A. A., Russell, L. M., Keene, W. C., and Kieber, D. J.: Contribution of sea surface carbon pool to organic matter enrichment in sea spray aerosol, *Nat. Geosci.*, 7, 228–232, <https://doi.org/10.1038/ngeo2092>, 2014.
- Rinaldi, M., Fuzzi, S., Decesari, S., Marullo, S., Santoleri, R., Provenzale, A., von Hardenberg, J., Ceburnis, D., Vaishya, A., O’Dowd, C. D., and Facchini, M. C.: Is chlorophyll *a* the best surrogate for organic matter enrichment in submicron primary marine aerosol?, *J. Geophys. Res.-Atmos.*, 118, 4964–4973, <https://doi.org/10.1002/jgrd.50417>, 2013.
- Savoie, D. L., Arimoto, R., Keene, W. C., Prospero, J. M., Duce, R. A., and Galloway, J. N.: Marine biogenic and anthropogenic contributions to non-sea-salt sulfate in the marine boundary layer over the North Atlantic Ocean, *J. Geophys. Res.-Atmos.*, 107, 4356, <https://doi.org/10.1029/2001JD000970>, 2002.
- Schiffer, J. M., Mael, L. E., Prather, K. A., Amaro, R. E., and Grassian, V. H.: Sea Spray Aerosol: Where Marine Biology Meets Atmospheric Chemistry, *ACS Central Sci.*, 4, 1617–1623, <https://doi.org/10.1021/acscentsci.8b00674>, 2018.
- Sciare, J., Favez, O., Sarda-Estève, R., Oikonomou, K., Cachier, H., and Kazan, V.: Long-term observations of carbonaceous aerosols in the Austral Ocean atmosphere: Evidence of a biogenic marine organic source, *J. Geophys. Res.-Atmos.*, 114, <https://doi.org/10.1029/2009JD011998>, 2009.
- Shi, J., Gao, H., Qi, J., Zhang, J., and Yao, X.: Sources, compositions, and distributions of water-soluble organic nitrogen in aerosols over the China Sea, *J. Geophys. Res.-Atmos.*, 115, <https://doi.org/10.1029/2009JD013238>, 2010.
- Sun, Y. L., Zhang, Q., Schwab, J. J., Chen, W. N., Bae, M. S., Lin, Y. C., Hung, H. M., and Demerjian, K. L.: A case study of aerosol processing and evolution in summer in New York City, *Atmos. Chem. Phys.*, 11, 12737–12750, <https://doi.org/10.5194/acp-11-12737-2011>, 2011.
- Tang, J., Wang, J., Zhong, G., Jiang, H., Mo, Y., Zhang, B., Geng, X., Chen, Y., Tang, J., Tian, C., Bualert, S., Li, J., and Zhang, G.: Measurement report: Long-emission-wavelength chromophores dominate the light absorption of brown carbon in aerosols over Bangkok: impact from biomass burning, *Atmos. Chem. Phys.*, 21, 11337–11352, <https://doi.org/10.5194/acp-21-11337-2021>, 2021.
- Tang, J., Xu, B., Zhao, S., Li, J., Tian, L., Geng, X., Jiang, H., Mo, Y., Zhong, G., Jiang, B., Chen, Y., Tang, J., and Zhang, G.: Long-Emission-Wavelength Humic-Like Component (L-HULIS) as a Secondary Source Tracer of Brown Carbon in the Atmosphere, *J. Geophys. Res.-Atmos.*, 129, e2023JD040144, <https://doi.org/10.1029/2023JD040144>, 2024.
- Tang, J.: For ACP, OSF, <https://doi.org/10.17605/OSF.IO/YMJ3F>, 2026.
- Tian, M., Li, H., Wang, G., Fu, M., Qin, X., Lu, D., Liu, C., Zhu, Y., Luo, X., Deng, C., Abdullaev, S. F., and Huang, K.: Seasonal source identification and formation processes of marine particulate water soluble organic nitrogen over an offshore island in the East China Sea, *Sci. Total Environ.*, 863, 160895, <https://doi.org/10.1016/j.scitotenv.2022.160895>, 2023.
- Tripathee, L., Kang, S., Chen, P., Bhattarai, H., Guo, J., Shrestha, K. L., Sharma, C. M., Sharma Ghimire, P., and Huang, J.: Water-soluble organic and inorganic nitrogen in ambient aerosols over the Himalayan middle hills: Seasonality, sources, and transport pathways, *Atmos. Res.*, 250, 105376, <https://doi.org/10.1016/j.atmosres.2020.105376>, 2021.
- Tsagkaraki, M., Theodosi, C., Grivas, G., Vargiakaki, E., Sciare, J., Savvides, C., and Mihalopoulos, N.: Spatiotemporal variability and sources of aerosol water-soluble organic nitrogen (WSON), in the Eastern Mediterranean, *Atmos. Environ.*, 246, 118144, <https://doi.org/10.1016/j.atmosenv.2020.118144>, 2021.
- Violaki, K., Sciare, J., Williams, J., Baker, A. R., Martino, M., and Mihalopoulos, N.: Atmospheric water-soluble organic nitrogen (WSON) over marine environments: a global perspective, *Biogeosciences*, 12, 3131–3140, <https://doi.org/10.5194/bg-12-3131-2015>, 2015.
- Wang, G. H., Cheng, C. L., Huang, Y., Tao, J., Ren, Y. Q., Wu, F., Meng, J. J., Li, J. J., Cheng, Y. T., Cao, J. J., Liu, S. X., Zhang, T., Zhang, R., and Chen, Y. B.: Evolution of aerosol chemistry in Xi’an, inland China, during the dust storm period of 2013 – Part 1: Sources, chemical forms and formation mechanisms of nitrate and sulfate, *Atmos. Chem. Phys.*, 14, 11571–11585, <https://doi.org/10.5194/acp-14-11571-2014>, 2014.
- Wang, J., Jiang, H., Jiang, H., Mo, Y., Geng, X., Li, J., Mao, S., Bualert, S., Ma, S., Li, J., and Zhang, G.: Source apportionment of water-soluble oxidative potential in ambient total suspended particulate from Bangkok: Biomass burning versus fossil fuel combustion, *Atmos. Environ.*, 235, 117624, <https://doi.org/10.1016/j.atmosenv.2020.117624>, 2020.
- Xie, M., Chen, X., Hays, M. D., Lewandowski, M., Offenberg, J., Kleindienst, T. E., and Holder, A. L.: Light Absorption of Secondary Organic Aerosol: Composition and Contribution of Nitroaromatic Compounds, *Environ. Sci. Technol.*, 51, 11607–11616, <https://doi.org/10.1021/acs.est.7b03263>, 2017.
- Xing, J., Song, J., Yuan, H., Wang, Q., Li, X., Li, N., Duan, L., and Qu, B.: Water-soluble nitrogen and phosphorus in aerosols and dry deposition in Jiaozhou Bay, North China: Deposition velocities, origins and biogeochemical implications, *Atmos. Res.*, 207, 90–99, <https://doi.org/10.1016/j.atmosres.2018.03.001>, 2018.
- Xu, Y., Miyazaki, Y., Tachibana, E., Sato, K., Ramasamy, S., Mochizuki, T., Sadanaga, Y., Nakashima, Y., Sakamoto, Y., Matsuda, K., and Kajii, Y.: Aerosol Liquid Water Promotes the Formation of Water-Soluble Organic Nitrogen in Submicrometer Aerosols in a Suburban Forest, *Environ. Sci. Technol.*, 54, 1406–1414, <https://doi.org/10.1021/acs.est.9b05849>, 2020.
- Yu, X., Yu, Q., Zhu, M., Tang, M., Li, S., Yang, W., Zhang, Y., Deng, W., Li, G., Yu, Y., Huang, Z., Song, W., Ding, X., Hu, Q., Li, J., Bi, X., and Wang, X.: Water Soluble Organic Nitrogen (WSON) in Ambient Fine Particles Over a

- Megacity in South China: Spatiotemporal Variations and Source Apportionment, *J. Geophys. Res.-Atmos.*, 122, 13045–13060, <https://doi.org/10.1002/2017JD027327>, 2017.
- Yu, X., Pan, Y., Song, W., Li, S., Li, D., Zhu, M., Zhou, H., Zhang, Y., Li, D., Yu, J., Wang, X., and Wang, X.: Wet and Dry Nitrogen Depositions in the Pearl River Delta, South China: Observations at Three Typical Sites With an Emphasis on Water-Soluble Organic Nitrogen, *J. Geophys. Res.-Atmos.*, 125, <https://doi.org/10.1029/2019jd030983>, 2020.
- Zamora, L. M., Prospero, J. M., and Hansell, D. A.: Organic nitrogen in aerosols and precipitation at Barbados and Miami: Implications regarding sources, transport and deposition to the western subtropical North Atlantic, *J. Geophys. Res.-Atmos.*, 116, <https://doi.org/10.1029/2011JD015660>, 2011.
- Zhao, Y., Bao, Z., Long, X., Liu, Y., Han, Y., Meng, L., Zeng, X., Li, L., Qi, X., Li, Z., Peng, C., Zhang, L., Chen, M., Zhai, C., and Chen, Y.: Evolution of secondary organic aerosol under extremely high humidity conditions in urban areas of southwestern China: Formation and scavenging, *Atmos. Res.*, 327, 108318, <https://doi.org/10.1016/j.atmosres.2025.108318>, 2026.
- Zhou, S., Chen, Y., Paytan, A., Li, H., Wang, F., Zhu, Y., Yang, T., Zhang, Y., and Zhang, R.: Non-Marine Sources Contribute to Aerosol Methanesulfonate Over Coastal Seas, *J. Geophys. Res.-Atmos.*, 126, e2021JD034960, <https://doi.org/10.1029/2021JD034960>, 2021.
- Zhou, S., Chen, Y., Wang, F., Bao, Y., Ding, X., and Xu, Z.: Assessing the Intensity of Marine Biogenic Influence on the Lower Atmosphere: An Insight into the Distribution of Marine Biogenic Aerosols over the Eastern China Seas, *Environ. Sci. Technol.*, 57, 12741–12751, <https://doi.org/10.1021/acs.est.3c04382>, 2023.